

# Preliminary computations for a representative structural volume of nuclear containment buildings

L. Jason

*CEA Saclay, DEN/DM2S/SEMT/LM2S, Gif sur Yvette, France*

S. Ghavamian

*EDF R&D, Clamart, France*

A. Courtois

*EDF SEPTEN, Villeurbanne, France*

**ABSTRACT:** The behaviour of a Representative Structural Volume for containment buildings of 1300 and 1450 MWe nuclear power plants is studied. First computations are considered to investigate the fracture mode of the structure and especially the role of the prestressing tendons. Cables initiate the development of a localized mechanical damage and help its propagation. The preliminary computations also underline the need for an experimental validation to further investigate the issue of the mechanical degradation. That is why an experimental device is proposed and described. As the new structure is supposed to represent the containment building of a 1450 MWe nuclear power plant, new computations are carried out with the finite element code Cast3M. They confirm the key role of the prestressed tendons in the development of damage.

## 1 INTRODUCTION

In high-power French nuclear power plants (1300 and 1450 MWe), the concrete containment vessel represents the third passive barrier after the fuel cladding and the containment vessel of the reactor core (Fig. 1). It is responsible for the safety of the environment as it is supposed to prevent leakage in case of accidents. That is why it is carefully monitored. Integrity tests, consisting in an internal pressure inside the structure, are carried out every ten years to check the leakage rate (if any). As the gas transfer through concrete is directly influenced by the mechanical degradation (Picandet et al., 2001) and as experiments can be hardly carried out because of the difficult environmental conditions, numerical studies remain the most convenient way to understand the degradation process. That is why, for the last decade, Electricité de France (EDF) has launched several important civil engineering research and development programs, dedicated to the analysis of prestressed pressure containment vessel (PCCV) reactor building. These concern the elaboration of new constitutive laws for concrete, techniques of modelling and resolution algorithms. The validity of the models (damage (Mazars, 1984) and/or plasticity (Jason et al., 2006), fracture (Ngo & Scordelis, 1967)...) and more generally the methodology for non-linear calculation must be obtained by comparing their performances with experimental results (benchmarking (Ghavamian & Delaplace, 2003) for example).

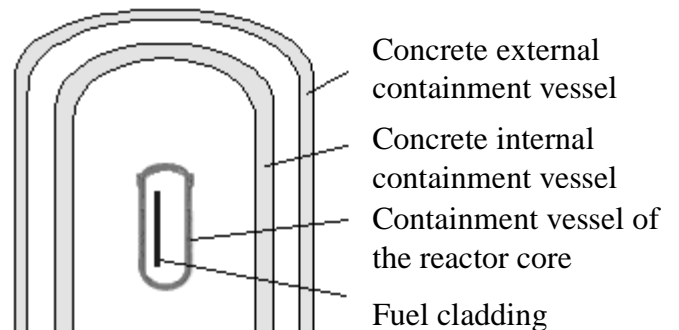


Figure 1. Barriers of a 1300 or 1450 MWe nuclear power plant.

The validation is generally obtained from simple tests on small size specimen, where elementary features of models are qualified. But more complex tests are also essential to determine the capacity of the calculations to predict the structural behaviour of more realistic and industrially representative cases.

In the field of nuclear containment buildings, a Representative Structural Volume (RSV) was designed. As the dimensions of containment vessels were not suitable for detailed studies, only one part was modelled. The RSV was designed to reproduce, as accurately as possible with acceptable computational costs, the behaviour of the typical part of the internal vessel. It contained concrete, passive steel bars and pretensioned cables. Preliminaries computations on this volume are presented in the section 2. At first the structure was considered as a mere numerical tool, to investigate the ability of constitutive laws to be applied on an industrial test. But unknowns about the role of the pretensioned tendons and mesh-dependency problems finally proved clearly that an experimental validation was

clearly that an experimental validation was necessary. That is why an experimental device was designed to validate, first qualitatively, then quantitatively, the tendencies that were observed through the parametric studies. Dimensions of the new structure and experimental processes are depicted in section 3.

As the new structure is supposed to represent the containment building of a 1450 MWe nuclear power plant, its dimensions and components are different from those of the preliminary RSV. That is why new computations have been carried out with the finite element code Cast3M at CEA (Cast3M, 2006) to evaluate the expected mechanical behaviour. The mode of fracture is especially highlighted in section 4 and a parametric study is also proposed to emphasize the mesh-dependency problem.

## 2 PRELIMINARY REPRESENTATIVE STRUCTURAL VOLUME

The application presented in this part has been proposed by Electricité de France in 2002. The test, named PACE 1300, is a Representative Structural Volume (RSV) of a PCCV of a French 1300 MWe nuclear power plant. Figure 2 illustrates the location of the RSV within the entire PCCV. The model incorporates almost all components of the real structure: concrete, vertical and horizontal reinforcement bars, transversal reinforcements, and pretensioned tendons in both horizontal and vertical directions. The size of the RSV is chosen to respect three conditions: large enough to include a sufficient number of components (and especially prestressed tendons) and to offer a significant observation area in the centre, far enough from boundary conditions, while remaining as small as possible to ease computations. The RSV includes 11 horizontal and 10 vertical reinforcement bars (on both internal and external faces), 5 horizontal and 3 vertical prestressed tendons, and 24 reinforcement hoops uniformly distributed in the volume. The geometry of the problem is given in figure 3. Figure 4 provides information about the steel distribution and properties.

The behaviour of the RSV needs to be as close as possible to the in situ situation. The following boundary conditions have thus been chosen: face SB blocked along the vertical direction, on face SH all nodes are restrained to follow the same displacement along Oz and no rotations are allowed for faces SG and SD (see figures 5 and 6).

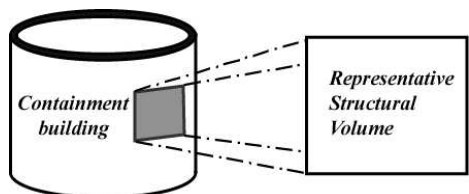


Figure 2. Position of the extracted Representative Structural Volume (RSV).

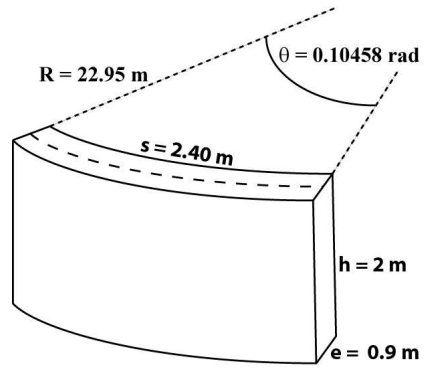
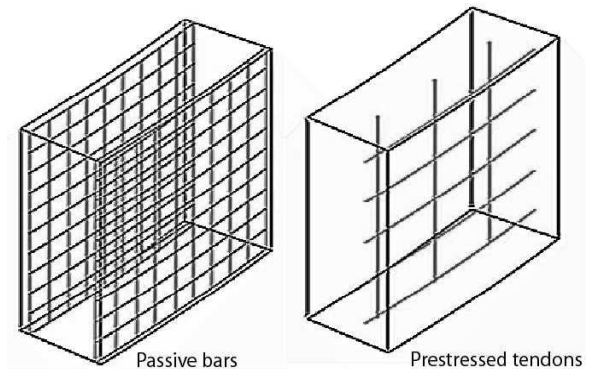


Figure 3. Geometry of the Representative Structural Volume (RSV).



Type	R m	e cm	D mm
Horizontal internal rebars	22.60	20	20
Horizontal external rebars	23.35	20	20
Vertical internal rebars	22.60	27.297	20
Vertical external rebars	23.35	27.170	20
Horizontal tendons	23.15	40.5	40.5
Vertical tendons	22.95	80	40.5
Hoops*	x	x	3.685

\* Hoops are uniformly distributed in the RSV

Figure 4. Steel geometries.

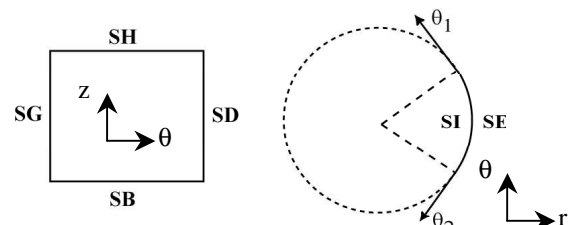
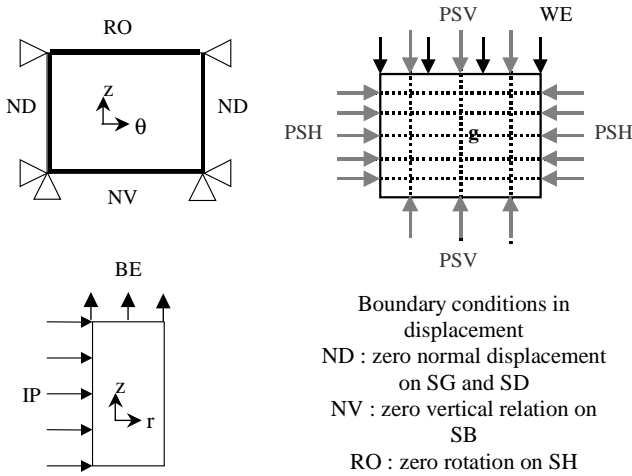


Figure 5. Definition of the Finite Element model indicating the boundary SG, SD, SH and SB.

In order to model the effect of the pretensioned tendons, bar elements are anchored to faces SG and SD for horizontal cables and to faces SB and SH for vertical tendons, then prestressed using internal forces.



Boundary conditions in stress  
PSH : horizontal prestress 5.28 MN per tendon  
PSV : vertical prestress 6.93 MN per tendon  
WE : weight of the surrounding structure 1.61 MPa  
g : gravity

Loading  
IP : internal pressure  
BE : tensile pressure proportional to the internal pressure (bottom effect)

Figure 6. Boundary conditions and loading for the RSV.

Then, these elements are restrained to surrounding concrete elements to represent the prestressing technology applied in French PPCVs.

The integrity test loading is represented by a radial pressure on the internal face SI and the bottom effect applied on face SH (tensile pressure proportional to the internal pressure to simulate the effect of the neighbouring structure). The self weight of the RSV and that of the surrounding upper-structure are also taken into account. With these conditions, a mesh containing 16,500 Hexa20 elements for concrete and 1200 bar element for reinforcement and tendons is used in this contribution.

Figure 7 provides the internal pressure applied on the volume as a function of the radial displacement of a point located at the bottom right of the internal face, using the elastic damage law developed by Mazars (1984). This curve can be divided in four parts. The initial state corresponds to the application of the prestress on the tendons.

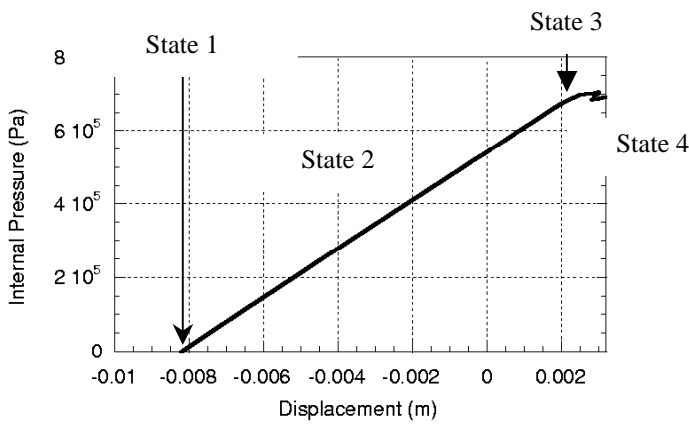


Figure 7. Displacement – pressure curve for the RSV.

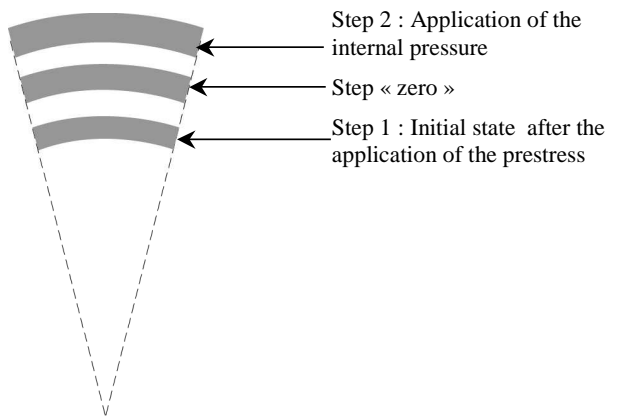


Figure 8. Radial deflection of the RSV through different steps (schematic). View from the top of the volume .

This yields a compaction of the volume and due to the boundary conditions (no normal displacement on the lateral face), it imposes an initial negative radial displacement (see figure 8). Then, upon application of the internal pressure, there is a zone of linear behaviour where the compaction is reduced and the structure returns towards its initial rest position before undergoing tension for higher values of internal pressure (almost 0.7 MPa). Damage does not evolve during state 2 but increases during state 3. Finally, a partial unloading of the volume appears (state 4) due to heavy cracking of the structure.

Figure 9 illustrates the evolution of the damage distribution during the simulation. Black points correspond to zones where the damage reaches a value up to 0.7. A first localization band appears in the middle of the volume along the vertical prestress tendon. Figure 10 presents the damage evolution with a view from the top of the RSV. The internal variable initiates from the middle of the structure along the vertical tendon then propagates along the horizontal pretensioned cables.

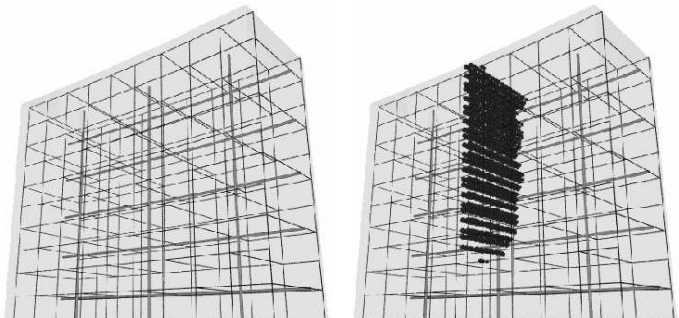


Figure 9. Development of a damage band in the RSV. Initial state (on the left) and damage band (on the right).

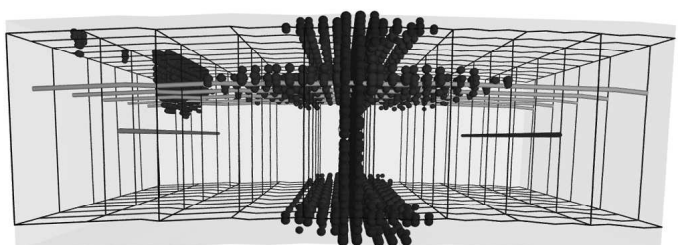


Figure 10. Development of the damage band. View from the top.

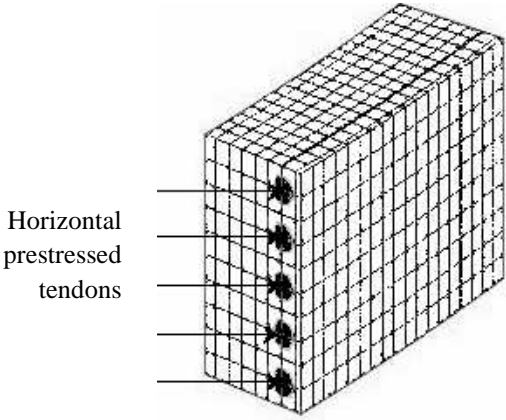


Figure 11. Damage distribution just after the prestress and before the application of the internal pressure.

Moreover, a “localization” of a small damage can also be observed along the horizontal pretensioned tendons, just after the prestress and before the application of the internal pressure (figure 11) (Jason, 2004). It is probably due to the boundary conditions, the steel-concrete interface (supposed perfect here) and/or the choice in the modelling (one dimensional bar elements in a three dimensional concrete volume).

These preliminaries computations show that the pretensioned tendons seem to play a key role in the development of the mechanical degradation. They are responsible for the initiation of the damage and help its propagation. But as these observations are up to now only based on numerical observations, further studies are needed. They clearly prove that an experimental validation is necessary to validate, first qualitatively, then quantitatively, the tendencies that have been observed through the computations.

### 3 EXPERIMENTAL PROGRAM

To validate the above-mentioned structural behaviour for prestressed reinforced concrete elements, an experimental program has been set up in association between EDF and the University of Karlsruhe. The test named PACE 1450 is quite similar to the PACE 1300 RSV described previously; the difference concerns the dimensions, reinforcement ratios and prestressing level. Since 1450 MW are obviously more than 1300 MW, thicker walls with more prestressing are required.

The precise purpose of the test is to validate computational models and techniques. To do so, within the specimen we shall create mechanical conditions as similar as possible to those of the real structure, and simulate a scenario where the containment vessel undergoes an uprising internal pressure. The aim is to follow the evolution of stress developed within the structure, and localise crack initiations and progression, which eventually could lead to microcracking of concrete and the decay in leakage tightness of the vessel. That is why the specimen will be

equipped with sound detection sensors and strain field measuring devices, both in the volume and on the surface of concrete.

To do so, the following experimental setup was imagined by the university of Karlsruhe (fig. 12):

- The specimen lays horizontally with its curvature pointing upwards.
- Hoop tendons apply their prestressing through steel abutments ('ears') to which they are anchored.
- A slight vertical prestressing is also applied.
- Internal vessel pressure is applied over the top surface of the specimen.
- The 8 hydraulic jacks stretch the specimen along hoop direction.

Loadings applied to the specimen will produce both radial displacement and membrane stretching of the specimen as in the real structure.

The structure will undergo several consecutive loading sequences, always applying the same internal pressure using dry air with normal humidity and temperature conditions. To encounter the aging effect of a real containment vessel, the prestressing is gradually reduced from 100% in RUN 1, down to 60% for RUN 4. This should produce more and more microcracks in concrete, and result in slight changes in structural permeability.

During the tests different kind of measures are recorded (fig. 13):

- Displacements of all 8 corners of the observation volume
- Volume strain field observation using Bragg fibre optic network cast in concrete
- Surface strain field observation using optical camera
- 3D localisation of cracking using sound detection sensors
- Gas leakage through a collecting chamber

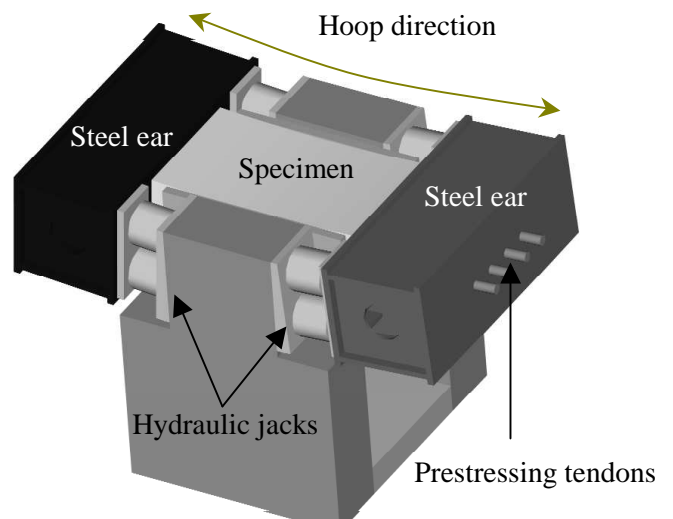


Figure 12. Experimental setup for the RSV.

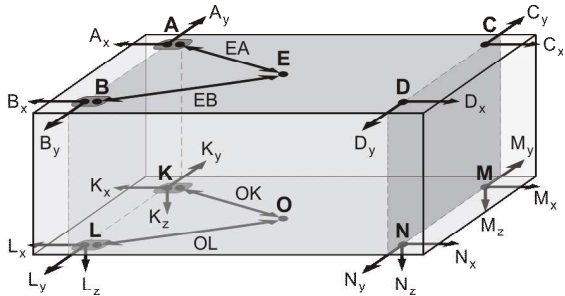


Figure 13. Position of displacement measurement devices.

Computational simulations will then be carried out by constraining the model to follow the displacements recorded at 8 corners of the model while prestressing and internal pressures are also applied. Then results will be compared to evaluate the possibility of the modelling to reproduce experimental observations.

#### 4 NEW PACE 1450 RSV

The dimensions, geometries, boundary conditions and loading are adapted from the definition of the experimental program. The new RSV includes 9 horizontal and 11 vertical reinforcement bars (on both internal and external faces), 4 horizontal and 1 vertical prestressed tendons. Hoops are not represented in the new RSV in order to simplify the model. The new geometry of the problem is given in figure 14. Figure 15 provides information about the steel distribution and properties.

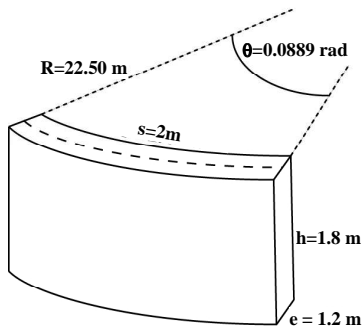
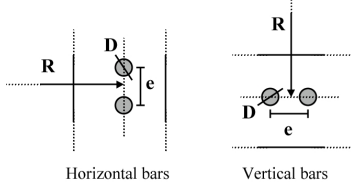


Figure 14. Dimensions of the new PACE 1450 RSV.

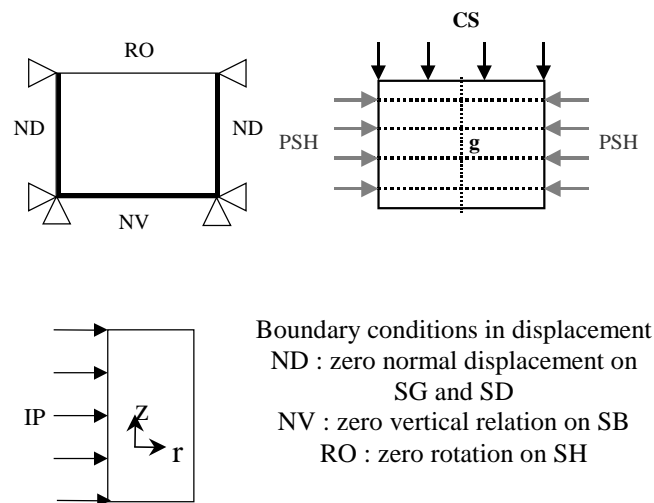


Type	R m	e cm	D mm
Horizontal internal reinf. bars	21.99	20	20
Horizontal external reinf. bars	23.02	20	20
Vertical internal reinf. bars	21.99	18	25
Vertical external reinf. bars	23.02	18	25
Horizontal tendons	22.50	40	84
Vertical tendon	22.15	-	84

Figure 15. Steel geometries of the new RSV.

The same boundary conditions as those chosen in the preliminary RSV are applied: face SB blocked along Oz, on face SH all nodes are restrained to follow the same displacement along Oz and no rotations are allowed for faces SG and SD. Only horizontal cables are prestressed as the vertical tendon is only cast to maintain the rigidity. Instead, a compressive homogeneous pressure of 1 MPa is applied during the prestressing on SH. The horizontal tension force is taken equal to 4.15 MN, which corresponds to a loss of 40 % of the initial 6.93 MN prestressing tension (simulation of the ageing process). For the sake of simplicity, the effect of gravity is not considered. Contrary to the preliminary computations, the bottom effect and the weight of the surrounding structure are not taken into account. Boundary conditions and loading are summarised in figure 16.

Figure 17 illustrates the radial displacement – pressure curve. It is still divided into four parts with an initial negative displacement due to the prestress, a zone of linear behaviour where damage does not evolve, then the apparition of a non linear response, followed by a partial unloading. Due to a change in the boundary and loading conditions, the admissible internal pressure is lower than in the initial RSV. The pressure – displacement curve is associated with different distributions of damage, as illustrated in figure 18. Two main phenomena are highlighted. First, a development of damage is observed from the inner surface of the volume.



Boundary conditions in displacement  
ND : zero normal displacement on SG and SD  
NV : zero vertical relation on SB  
RO : zero rotation on SH

Boundary conditions in stress  
PSH : horizontal prestress 4.15 MN per tendon  
CS : compressive stress 1 MPa

Loading  
IP : internal pressure

Figure 16. Boundary conditions and loading for the new RSV.

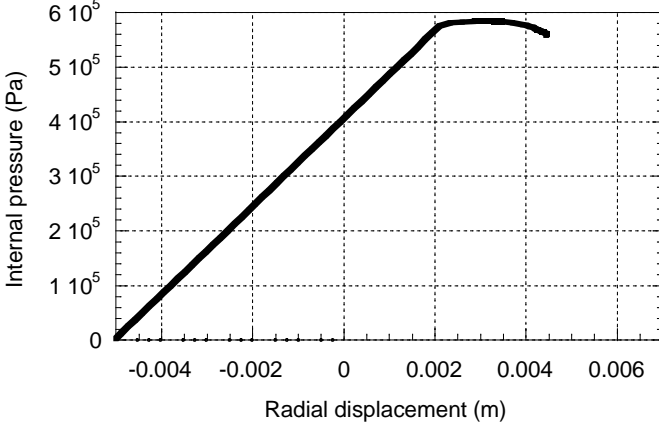


Figure 17. Radial displacement – internal pressure curve for the new RSV.

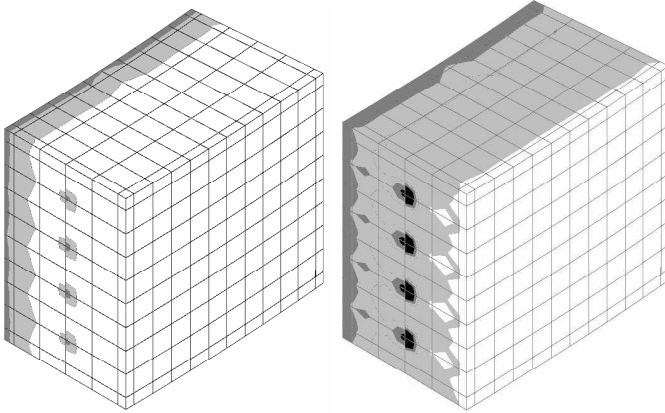


Figure 18. Evolution of the damage distribution in the new RSV after the application of an internal pressure.

It was expected since the loading is an internal pressure inside part of a cylinder. More interesting is the initiation and development of damage along the horizontal prestressed tendons. The internal variable indeed appears along the cables then propagates from the cables to the rest of the structure. It shows that the tendons play a key role in the damage distribution.

In comparison with the preliminary RSV, the mechanical mode of degradation is totally different, as we do not observe the localisation of strains or damage any more (due to a change in the loading conditions and especially the tensile bottom effect which is not taken into account any more). Moreover, in the present case, the level of prestress does not impose enough compression to create damage without internal pressure, as observed in figure 11 for the first RSV. Nevertheless, some similarities are also noticed about the role of the tendons. In both cases, they initiate, partly (new RSV) or totally (preliminary RSV) the evolution of damage and help its propagation.

The last step of these preliminary computations consists in investigating the mesh-dependency of the response. To this aim, two meshes, with different densities, are considered (figure 19). The value of the maximum of the equivalent strain is compared for elastic and nonlinear computations.

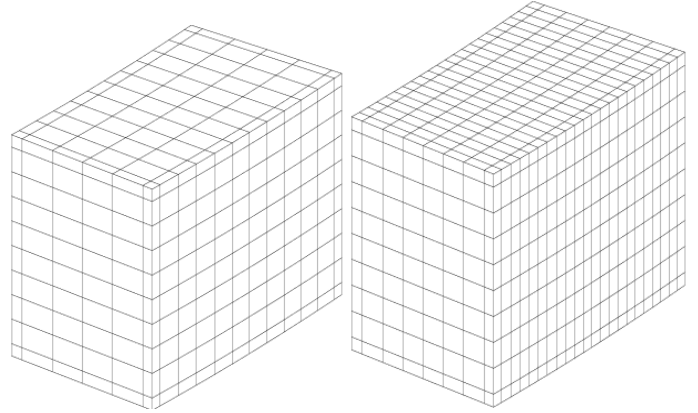


Figure 19. Meshes for the mesh-dependency study.

The equivalent strain, defined by Mazars (1984) quantified the tensile strains that are responsible for the development of the mechanical damage.

$$\varepsilon_{eq} = \sqrt{\sum_{i=1}^3 (\langle \varepsilon_i \rangle_+)^2} \quad (1)$$

$\langle \varepsilon_i \rangle_+$  represents the positive principal values of the strain tensor.

To emphasize the role of the prestress, a computation with a tension of 6.93 MN is also carried out (initial tension in the cables if the ageing process is not taken into account).

Table 1. Mesh-dependency studies. Difference between the maximum of the equivalent strain for the coarse mesh and the medium mesh

	Prestress 6.93 MN	Prestress 4.15 MN
Elastic computation	16 %	0.03 %
Non linear computation	19 %	2.46 %

The mesh-dependency problem that appears in the non linear computation can be partly explained by the strain and damage localization. It is an usual effect of softening laws (Crisfield, 1982) and could need the use of a regularization technique (Pijaudier-Cabot & Bazant, 1987), that will not be discussed in this contribution. More interesting is the dependency observed during the elastic computation. As the constitutive law is elastic, only the material components can explain this effect. If we compare the calculation with 6.93 MN and 4.15 MN prestresses, it can be noticed that the higher the pretension is, the more important the mesh-dependency becomes. The application of prestress thus triggers a local mesh-dependency, probably due to the one-dimensional representation of the cables into a three dimensional volume (localization of the application of the tension force).

## 5 CONCLUSIONS

Different preliminary computations have been carried out to characterize the mechanical behavior of a Representative Structural Volume of a containment building of 1300 and 1450 MWe nuclear power plant. The role of the prestress tendons is especially underlined. They are partly responsible for the initiation of damage and help its propagation. Moreover, from a numerical point of view, they seem responsible for a mesh-dependency problem that even appears for elastic computations.

These observations require an experimental validation, that will start soon, to validate the role of the prestress and also the need for further numerical studies to understand the influence of the one-dimensional modelling of the pretensioned cables. This issue will be investigated by comparing the present results with a full three dimensional analysis (discretization of the cables with 3D elements, figure 20)

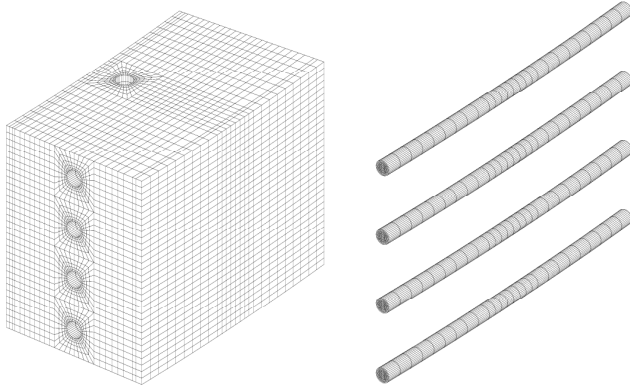


Figure 20. Mesh for future computations. Discretization of the cables with full 3D elements.

## REFERENCES

- Cast3M. 2006. Description of the finite element code Cast3M. <http://www-cast3m.cea.fr>.
- Crisfield M.A. 1982. Local instabilities in the non linear analysis of reinforced concrete beams and slabs, *Proceedings of the Institution of Civil Engineers* 73:135-145
- Ghavamian, S. & Delaplace, A. 2003. Modèles de fissuration de béton. Projet MECA. *Revue Française de Génie Civil*, 7, 5
- Jason, L. Huerta, A. Pijaudier-Cabot, G. & Ghavamian, S. 2006. An elastic plastic damage formulation for concrete: application to elementary and comparison with an isotropic damage model. *Computer Methods in Applied Mechanics and Engineering*. 195, 52:7077-7092
- Jason, L. 2004. *Relation endommagement perméabilité pour les bétons. Application aux calculs de structures*. PhD Thesis, Nantes, Université de Nantes et Ecole Centrale de Nantes, France
- Mazars, J. 1984. *Application de la mécanique de l'endommagement au comportement non linéaire et à la rupture du béton de structure*. PhD thesis. Paris, Université Paris VI, France
- Ngo, D. & Scordelis, A.C. 1967. Finite element analysis of reinforced concrete beams. *Journal of the American Concrete Institute*. 64 : 152-163
- Picandet, V. Khelidj, A. Bastian, G. 2001. Effect of axial compressive damage on gas permeability of ordinary and high performance concrete. *Cement and Concrete Research*. 31:1525-1532.
- Pijaudier-Cabot, G. & Bazant Z.P. 1987. Nonlocal damage theory. *Journal of Engineering Mechanics*. 113:1512-1533.